Systems & Control Transactions

Original Research Article
Peer Reviewed Conference Proceeding
ESCAPE 36 - European Symposium on Computer Aided Process Engineering
Sheffield, UK. 21-24 June 2026

PSE PRESS

Optimal Operation of an Alkaline Electrolyzer in an Industrial Setting Using Effective Linearization Techniques

Jonaed Bin Mustafa Kamal[a]*, Loukas Kyriakidis[a], Saskia Bublitz[a], Bogdan Dorneanu[b], and Harvey Arellano-Garcia[b]

[a] German Aerospace Center, Institute of Low-Carbon Industrial Processes, Simulation and Virtual Design, Cottbus, Germany
[b] Brandenburg University of Technology, Chair of Process and Plant Technology, Cottbus, Germany
* Corresponding Author: jonaed.mustafakamal@dlr.de.

ABSTRACT

Renewable powered water electrolysis offers a promising strategy to decarbonize industrial sectors with high demand for hydrogen. Operational optimization of industrial electrolyzer systems is often formulated as mixed-integer linear programming (MILP) problems, where a constant hydrogen production to electrical power consumption ratio is assumed instead of the nonlinear relationship. Incorporating a nonlinear electrolyzer model into a linear optimal hydrogen dispatch framework remains a significant challenge. This study addresses this challenge by formulating the optimization problem in two ways. First, the model is solved as a nonlinear programming (NLP) problem by incorporating a nonlinear model of an alkaline electrolyzer (AEL) into the optimization framework. The binaries and integers are relaxed to continuous variables and associated penalty terms are added to the objective function to enforce integrality. The NLP is solved using the local nonlinear solver Interior Point OPTimizer (IPOPT) using a multi-start approach, where the solver is executed from random initial points and the minimum objective value is taken as the best guess for the global minimum. Second, a linearized model of the AEL is used in an MILP formulation. The univariate nonlinear terms within the model are approximated using three piecewise linearization techniques, i.e., convex combination, convex combination with SOS2 variables and a slope based big-M formulation. The bilinear terms are relaxed using the McCormick envelope. Results show that the MILP formulation achieves faster solution times, with varying accuracy depending on the linearization method, whereas the NLP approach more accurately captures the hydrogen production curve, albeit having longer convergence times.

Keywords: Alkaline electrolyzer, Renewable hydrogen system, Piecewise linearization, McCormick relaxation, Operational optimization

INTRODUCTION

Optimal dispatch problems for electrolysis require robust and quickly solvable process models to enable real-time control decisions. For this reason, mixed-integer linear programming (MILP) models are often employed [1-3]. Among the simplest models are those assuming a constant electrolyzer efficiency or a fixed hydrogen production to electrical power consumption ratio. Baumhof et al. [4] showed that such models exhibit significant deviations in the partial load range of the electrolyzer resulting in sub-optimal solutions. In fact, there exists a nonlinear relationship between power consumption and hydrogen production that can be modeled using detailed physical models or semi-empirical models of the electrolyzer [5]. Baumhof et al. [4] incorporated the widely adopted semi-empirical model of an alkaline electrolyzer (AEL) first proposed by Ulleberg [6] and later extended by Sánchez et al. [7] into their MILP framework by piecewise linearizing the power consumption vs hydrogen production curve obtained from a separate nonlinear AEL model. Furthermore, the study builds the MILP by introducing different operational states, i.e., on, off and stand-by, of the AEL.

Due to the inherent complex nature, incorporating a nonlinear component model into a linear optimization problem remains a challenge. On one hand nonlinear solvers like Interior Point OPTimizer (IPOPT) only works

with continuous variables [8] and thus cannot handle integers and binary variables. On the other hand linear solvers only work with linear objective function and linear constraints [9]. This study incorporates the nonlinear AEL model into a linear operational optimization problem by first solving the problem as a nonlinear program (NLP), where the integer and the binary variables are relaxed to continuous variables and associated penalty terms are added to the objective function to enforce integrality. Second, the problem is reformulated as an MILP by linearizing the univariate nonlinear terms within the AEL model using three different piecewise linearization techniques, and relaxing the multilinear terms using McCormick envelope. Furthermore, this paper extends the work of Baumhof et al. [4] by developing an AEL system model tailored to a multi-stack configuration. This work is part of the development of a digital twin for a renewable powered 40 MW AEL system designed to supply hydrogen to a refinery in Corinth, Greece within the framework of the EU project EPHYRA [10].

The paper has two primary objectives. First, it tries to identify the best linearization method when linearizing the nonlinear semi-empirical AEL model when applied to a hydrogen dispatch problem, evaluating performance in terms of accuracy and computational speed. Second, it compares the results of the MILP with the NLP to assess the merits of each approach and evaluates if the linearized model can accurately reproduce the variable trajectories when compared to the NLP formulation.

DESCRIPTION OF THE SYSTEM

The industrial system, illustrated in **Figure 1**, has a 40 MW pressurized AEL at its core that produces hydrogen for a refinery. The AEL is primarily powered by a photovoltaic (PV) plant, with supplementary power produced through waste heat recovery from the refinery via an Organic Rankine Cycle (ORC). When required, power can be drawn from the grid for meeting additional hydrogen demand. The AEL system is divided into 8 stacks with each operating at a pressure of 20-25 bar and consuming 5 MW power when operating at full capacity. The produced hydrogen is compressed and routed through a hydrogen storage system operating at 350 bar before being delivered to the refinery. The system operates in such a way that it meets the hydrogen demand of the refinery at each time step.

MODEL FORMULATION

The optimal hydrogen dispatch problem is first formulated as a mixed-integer nonlinear problem (MINLP) and solved as an NLP by relaxing the binary and integer variables to continuous variables and then introducing penalty terms within the objective function to encourage integrality. Then it is converted to an MILP by linearizing the nonlinear terms within the AEL model. The optimization framework is implemented in the Python based optimization framework Pyomo. The NLP is solved using the local nonlinear solver Interior Point OPTimizer (IPOPT), whereas the MILP formulation is solved using the linear solver Gurobi. The objective function and the constrains within the optimization problem are described in detail in the following paragraphs.

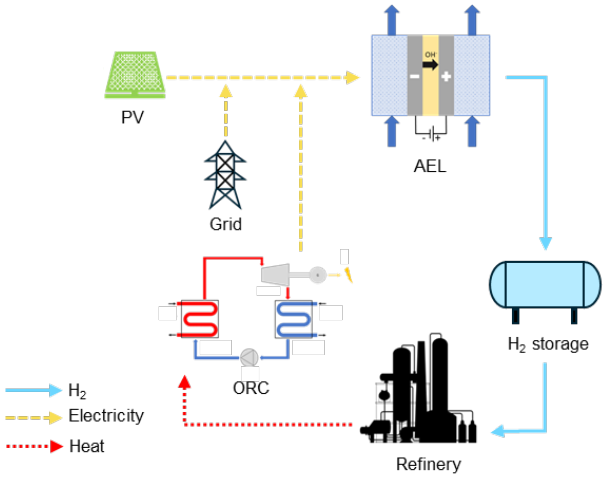

Figure 1. Process flow diagram of the industrial setup.

Objective function

The objective of the optimization problem is to minimize the total operating costs associated with the system over a period of n hours. The objective function is thus formulated as:

$$\min \sum_{t=1}^{n} \left[P_{\text{grid}}^{t} c_{\text{grid}}^{t} + \sum_{s=1}^{N_{\text{stack}}} z_{\text{su}}^{t,s} c_{\text{su}} \right] \quad (1)$$

where, P_{grid} is the power drawn from the grid, c_{grid} the cost to purchase one unit of grid electricity, z_{su} a binary variable denoting the start-up of one AEL stack, discussed in detail in the following section, c_{su} the cost associated with the start-up of a stack, n the total number of time steps, and N_{stack} the total number of stacks. The superscripts t and s are the time step and the AEL stack indices and are used throughout the model. The objective function in the NLP adds further penalty terms for enforcing integrality of the binary and the integer variables.

Operational States of the AEL Stacks

The operational states of the AEL stacks are modeled in a similar way to Baumhof et al. [4]. However, in this work, the model is further extended to be compatible with a multi-stack AEL system. Each stack has three operational states, i.e., on, off and standby. These operational states are described by the three binary variables $z_{\text{on}}, z_{\text{off}}$, and z_{sb}. At any time step, only one of the states can be active, which can be written as:

$$z_{\text{on}}^{t,s} + z_{\text{off}}^{t,s} + z_{\text{sb}}^{t,s} = 1 \quad (2)$$

The cold start-up of a stack is indicated by the binary variable z_{su}. The variable z_{su} is 0 at the start and becomes 1 whenever transitioning from off to on state between two consecutive time steps. The constraints are thus written as:

$$z_{\text{su}}^{t=1,s} = 0 \quad (3)$$

$$z_{\text{su}}^{t,s} \geq z_{\text{on}}^{t,s} - z_{\text{on}}^{t-1,s} - z_{\text{sb}}^{t-1,s} \text{ for } t = 2, \ldots, n \quad (4)$$

An additional constraint is added to avoid a stack from transitioning from off to standby state:

$$z_{\text{off}}^{t-1,s} + z_{\text{sb}}^{t,s} \leq 1 \text{ for } t = 2, \ldots, n \quad (5)$$

AEL Model

The AEL is modeled using the widely adopted semi-empirical model proposed first by Ulleberg [6] and later extended by Sánchez et al. [7]. For brevity, only the equations that were linearized are mentioned in this paper.

The reversible cell voltage of an AEL cell can be written as:

$$U_{\text{rev}}^{t,s} = U_{\text{rev0}}^{t,s} + \frac{RT_{\text{stack}}^{t,s}}{2F} \ln\left(\frac{(p_{\text{cell}}^{t,s} - p_{\text{H}_2\text{O}})^{1.5}}{\alpha_{\text{H}_2\text{O}}}\right) \quad (6)$$

where, U_{rev} is the reversible cell voltage, U_{rev0} the standard reversible cell voltage, T_{stack} the stack temperature, F the Faraday number, p_{cell} the cell pressure, $p_{\text{H}_2\text{O}}$ the partial vapor pressure, and $\alpha_{\text{H}_2\text{O}}$ the water activity. The cell voltage U_{cell} is expressed as:

$$U_{\text{cell}}^{t,s} = U_{\text{rev}}^{t,s} + K_1 \frac{I_{\text{cell}}^{t,s}}{A_{\text{cell}}} + s\log\left(K_2 \frac{I_{\text{cell}}^{t,s}}{A_{\text{cell}}} + 1\right) \quad (7)$$

where, I_{cell} is the cell current, A_{cell} the cell area, and s an empirical coefficient. K_1 and K_2 are two nonlinear terms that are dependent on T_{stack}. The Faraday efficiency η_{Faraday} is calculated as:

$$\eta_{\text{F}}^{t,s} = B_1 + B_2 \exp\left(K_3 \frac{A_{cell}}{I_{cell}^{t,s}}\right) \quad (8)$$

where, η_{F} is the Faraday efficiency, B_1 and B_2 two empirical coefficients, and K_3 a nonlinear term that depends on T_{stack}. At each time step, the total amount of hydrogen produced by an AEL stack $\dot{m}_{\text{prod, st}}$ is described by the Faraday law as:

$$\dot{m}_{\text{prod, st}}^{t,s} = \frac{\eta_{\text{F}}^{t,s} I_{\text{cell}}^{t,s}}{2F} M_{H_2} N_{\text{cell}} z_{\text{on}}^{t,s} \quad (9)$$

where, N_{cell} is the number of cells in the stack, and M_{H2} the molar mass of hydrogen. The total amount of hydrogen produced $\dot{m}_{\text{prod}}$ is the summation of the hydrogen produced by each stack:

$$\dot{m}_{\text{prod}}^{t} = \sum_{s=1}^{N_{\text{stack}}} \dot{m}_{\text{prod, st}}^{t,s} \quad (10)$$

The power consumed by an AEL stack P_{stack} can be written as:

$$P_{\text{stack}}^{t,s} = N_{\text{cell}} U_{\text{cell}}^{t,s} I_{\text{cell}}^{t,s} z_{\text{on}}^{t,s} + P_{\text{sb}} z_{\text{sb}}^{t,s} \quad (11)$$

where, U_{cell} is the cell voltage that is assumed to be same for all the cells in a stack, and P_{sb} the power consumed by a stack in its standby state. P_{stack} has to be between the maximum capacity P_{cap} and the minimum load P_{min} of the stack:

$$P_{\text{stack}}^{t,s} \leq P_{\text{cap}} z_{\text{on}}^{t,s} + P_{\text{sb}} z_{\text{sb}}^{t,s} \quad (12)$$

$$P_{\text{stack}}^{t,s} \geq P_{\text{min}} z_{\text{on}}^{t,s} + P_{\text{sb}} z_{\text{sb}}^{t,s} \quad (13)$$

Constraints (6) to (8) were approximated using a composite linearization approach, where piecewise approximation [11] and the McCormick envelope method [12] were used sequentially. Furthermore, the multilinear terms in equations (9) and (11) were relaxed using the same McCormick relaxation. The linearization methods used in this study are discussed in detail in the next section.

Power Balance

At every time step, the power balance of the whole system can be expressed by:

$$P_{\text{PV}}^{t} + P_{\text{ORC}}^{t} + P_{\text{grid}}^{t} = P_{\text{e}}^{t} + P_{\text{comp}}^{t} \quad (14)$$

where, P_{PV} is the power produced by the PV plant, P_{ORC} is the power produced by the ORC, P_{e} is the total power consumed by the AEL system, and P_{comp} is the power consumed by the hydrogen storage compressor. P_{e} is the summation of the power consumption of each stack, expressed as:

$$P_{\text{e}}^{t} = \sum_{s=1}^{N_{\text{stack}}} P_{\text{stack}}^{t,s} \quad (15)$$

P_{comp} is a function of the specific power consumption of the compressor w_{comp} and the storage inlet mass flow rate $\dot{m}_{\text{sto, in}}$ [13]. To keep the model simple, w_{comp} is taken as a constant parameter. Therefore, the constraint is written as:

$$P_{\text{comp}}^{t} = w_{\text{comp}} \dot{m}_{\text{sto, in}}^{t} \quad (16)$$

P_{PV} is modeled as a function of solar irradiance and module efficiency [14]. The polynomial equation to calculate P_{ORC}, expressed as a function of the temperature of the heat source and the cooling air (ambient) temperature, was obtained from the manufacturer of the ORC unit while the heat source temperature data were provided by the refinery.

Mass Balance

The mass balance of the system at every time step is written as:

$$\dot{m}^t_{\text{prod}} = \dot{m}^t_{\text{d}} + \dot{m}^t_{\text{sto, in}} - \dot{m}^t_{\text{sto, out}} \quad (17)$$

where, $\dot{m}_{\text{prod}}$ is the total hydrogen produced, $\dot{m}_{\text{d}}$ the hydrogen demand, and $\dot{m}_{\text{sto, out}}$ the mass flow rate of the hydrogen exiting the storage.

Hydrogen Storage

The operation of the hydrogen storage at each time step can be expressed by the following two constraints:

$$m^t_{\text{sto}} = m^{t-1}_{\text{sto}} + (\dot{m}^t_{\text{sto, in}} - \dot{m}^t_{\text{sto, out}})\Delta t \quad (18)$$

$$m^{t=0}_{\text{sto}} = m_{\text{sto, ini}} \quad (19)$$

where, m_{sto} is the amount of stored hydrogen at any time step, and $m_{\text{sto, ini}}$ is the amount of hydrogen stored at the start of the operation. Both $\dot{m}_{\text{sto, in}}$ and $\dot{m}_{\text{sto, out}}$ are limited by the maximum inlet and outlet flowrates of the storage, $\dot{m}_{\text{sto, in, max}}$ and $\dot{m}_{\text{sto, out, max}}$, respectively:

$$\dot{m}^t_{\text{sto, in}} \leq \dot{m}_{\text{sto, in, max}} \quad (20)$$

$$\dot{m}^t_{\text{sto, out}} \leq \dot{m}_{\text{sto, out, max}} \quad (21)$$

The maximum amount of stored hydrogen is limited by the volumetric storage capacity $V_{\text{sto, max}}$ and is given by:

$$m^t_{\text{sto}} \leq V_{\text{sto, max}} \rho_{H_2} \quad (22)$$

where, the density of hydrogen, ρ_{H_2}, is calculated using the standardized equation for hydrogen gas density, given in [15]. Two further constraints are added to prevent the storage from being charged and discharged at the same time:

$$\dot{m}^t_{\text{sto, in}} \leq z^t_{\text{ch}} \dot{m}_{\text{sto, in, max}} \quad (23)$$

$$\dot{m}^t_{\text{sto, out}} \leq (1 - z^t_{\text{ch}}) \dot{m}_{\text{sto, out, max}} \quad (24)$$

where, z_{ch} is a binary variable indicating the charging of the storage.

LINEARIZATION METHODS

The nonlinearities in the optimization problem, described by equation (1) to (24), can be divided into two categories. The first category contains the univariate nonlinear terms that are linearized using piecewise linear approximation methods. Three different piecewise linearization techniques [11] are implemented and are discussed below. The second category consists of the multilinear terms, i.e. the bilinear and trilinear terms, that are approximated by the McCormick relaxation [12].

Piecewise Linearization Methods

Convex combination (CC)

A nonlinear function $f(x)$ is approximated by discretizing the domain of x into $k-1$ segments with k being the number of breakpoints. The linear approximations of x and $f(x)$ are weighted sums (convex combination) of their values at the breakpoints, where the weights λ_i sum to 1. In (29) to (32), the binary variables z_i ensure that at most two adjacent λ_i can be non-zero. The convex combination method can be written as:

$$f = \sum_{i=1}^{k} f(x_i)\lambda_i \quad (25)$$

$$x = \sum_{i=1}^{k} x_i \lambda_i \quad (26)$$

$$\lambda_i \geq 0 \quad (27)$$

$$\sum_{i=1}^{k} \lambda_i = 1 \quad (28)$$

$$\sum_{i=1}^{k-1} z_i = 1 \quad (29)$$

$$\lambda_1 \leq z_1 \quad (30)$$

$$\lambda_i \leq z_{i-1} + z_i \text{ for } i = 2, \dots, k-1 \quad (31)$$

$$\lambda_k \leq z_{k-1} \quad (32)$$

Convex combination with SOS2 variables (CC-SOS2)

To avoid the use of binary variables z_i, as seen in (29) to (32), the set of variables $\{\lambda_1, \lambda_2, \dots, \lambda_n\}$ can be formulated as a Special Ordered Set of type 2 (SOS2), which ensures the adjacency rule of the λ_i variables. With $\lambda_i \in$ SOS2, the formulation is then fully described by (24) to (27). It has to be noted that a suitable solver capable of handling SOS2 variables needs to be chosen.

Slope based Big-M formulation

To avoid the use of continuous variables λ_i in (25) to (32), the nonlinear function $f(x)$ can be approximated using a big-M formulation. Constraints (33) and (34) restrict the variable x to lie within the active segment, while (35) and (36) employ a Big-M formulation to define the function value f by the slope and the intercept of the selected segment.

$$x \geq x_i - (1 - z_i)(x_{\max} - x_{\min}) \quad (33)$$

$$x \leq x_{i+1} + (1 - z_i)(x_{\max} - x_{\min}) \quad (34)$$

$$f \geq a_i x + b_i - (1 - z_i)M \quad (35)$$

$$f \leq a_i x + b_i + (1 - z_i)M \quad (36)$$

$$\sum_{i=1}^{k-1} z_i = 1 \quad (37)$$

where, $a_i = \frac{f(x_{i+1}) - f(x_i)}{x_{i+1} - x_i}$, and $b_i = f(x_i) - a_i x_i$. M is a sufficiently large positive constant used to activate or deactivate constraints (35) and (36).

McCormick Relaxation

The McCormick envelope relaxes the product of two continuous variables, $w = xy$, where $x \in [x_{\text{lb}}, x_{\text{ub}}]$ and $y \in [y_{\text{lb}}, y_{\text{ub}}]$, by defining the convex hull of the feasible set through the following linear inequalities:

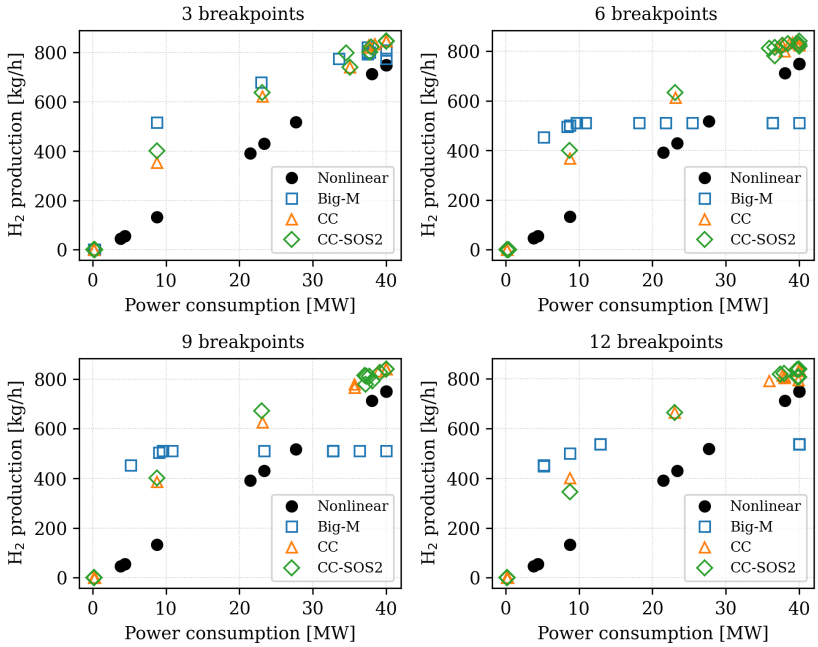

Figure 2. Hydrogen production-power consumption curve: NLP vs. MILP formulations using different linear approximation methods with 3 breakpoints (**top left**), 6 breakpoints (**top right**), 9 breakpoints (**bottom left**) and 12 breakpoints (**bottom right**).

$$w \geq x_{\text{lb}} y + y_{\text{lb}} x - x_{\text{lb}} y_{\text{lb}} \tag{38}$$

$$w \geq x_{\text{ub}} y + y_{\text{ub}} x - x_{\text{ub}} y_{\text{ub}} \tag{39}$$

$$w \leq x_{\text{ub}} y + y_{\text{lb}} x - x_{\text{ub}} y_{\text{lb}} \tag{40}$$

$$w \leq x_{\text{lb}} y + y_{\text{ub}} x - x_{\text{lb}} y_{\text{ub}} \tag{41}$$

If the bilinear term consists of a continuous variable $x \in [x_{\text{lb}}, x_{\text{ub}}]$ and a binary variable $z \in \{0,1\}$, the McCormick relaxation reduces to the following inequalities:

$$x_{\text{lb}} z \leq w \leq x_{\text{ub}} z \tag{42}$$

$$x - x_{\text{ub}}(1-z) \leq w \leq x - x_{\text{lb}}(1-z) \tag{43}$$

RESULTS

The NLP is solved using a multi-start approach using the local nonlinear solver IPOPT, in which the optimization problem is executed 50 times from random initial points and the solution with the minimum objective value is taken as the best guess for the global minimum. The MILP is solved with the linear solver Gurobi using the three piecewise linearization methods, described in the section above, by gradually increasing the number of breakpoints to potentially enhance the accuracy of the decision variables. The optimization was done over a 15-hour period. The dimensions of the different formulations are listed in **Table 1**. All the simulations were run using a computer with a 13th Gen Intel(R) Core(TM) i7-1365U processor.

Table 1: Dimensions of the MILP formulations and the NLP

Method	Variable count	Constraint count
CC (3 breakpoints)	8040	11257
CC (6 breakpoints)	12360	13417
CC (9 breakpoints)	16680	15577
CC (12 breakpoints)	21000	17737
CC-SOS2 (3 breakpoints)	6600	8377
CC-SOS2 (6 breakpoints)	8760	8377
CC-SOS2 (9 breakpoints)	10920	8377
CC-SOS2 (12 breakpoints)	13080	8377
Big-M (3 breakpoints)	5880	12457
Big-M (6 breakpoints)	8040	21097
Big-M (9 breakpoints)	10200	29737
Big-M (12 breakpoints)	12360	38377
NLP	2655	2287

We first assess the accuracy of the linearization methods by comparing the hydrogen production curve (hydrogen production versus power consumption) obtained from the MILP formulations using the three linearization methods with that of the NLP. Given that the NLP formulation retains the original nonlinear model, we take the hydrogen production curve from the NLP as the reference. We see from **Figure 2** that the curves from all of

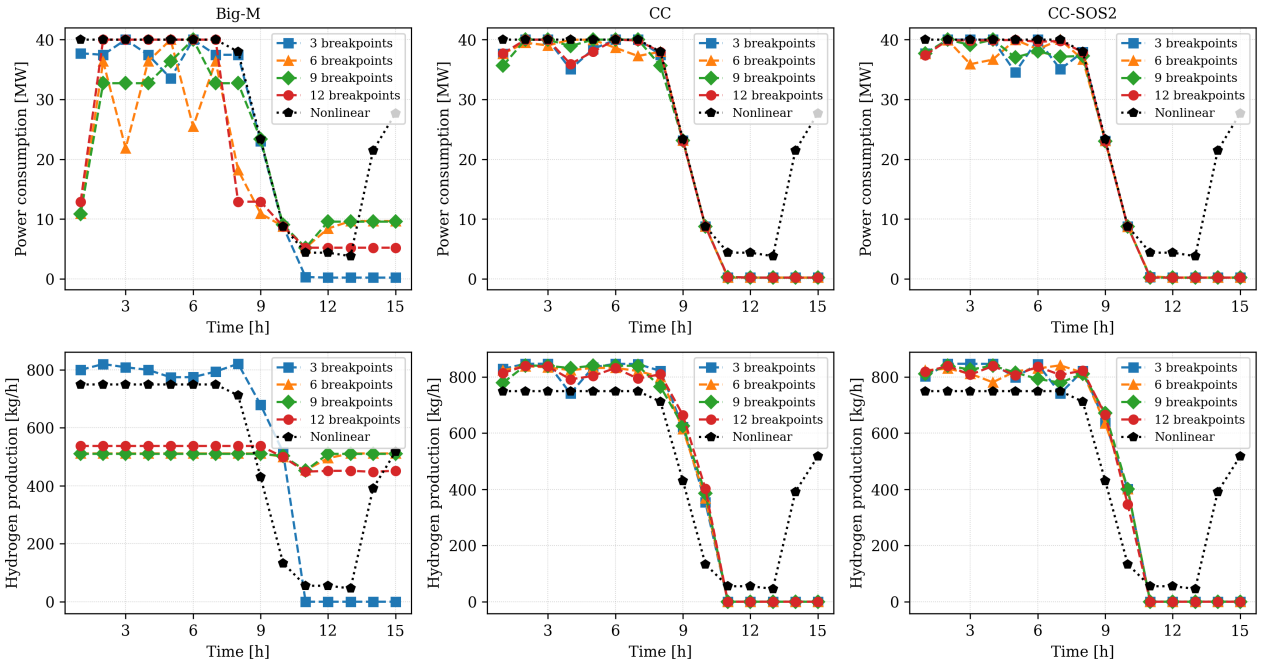

Figure 3. Power consumption (**top**) and hydrogen production (**bottom**) profiles: MILP formulations with different linearization methods vs. NLP.

the MILP formulations deviate from that of the NLP, but to varying degree. As expected, the CC and the CC-SOS2 produce very similar results since their underlying principles are the same. The performance of the big-M formulation heavily depends on the choice of the big-M parameter, which is difficult to appropriately determine. As a rule of thumb, the big-M was initially set equal to the difference between the maximum and minimum values of the nonlinear function being linearized. While this was sufficiently large for three breakpoints, the big-M value had to be increased every time the number of breakpoints was increased to prevent infeasibility, causing the feasible region to increase resulting in loose relaxation. Consequently, the big-M linearization method exhibits larger deviation in the hydrogen production curve as the number of breakpoints increases. This is also evident in **Figure 3**, where we see that beyond three breakpoints, the big-M formulation produces unusable results. Due to the difficulty in choosing an adequately large value of big-M, we come to the conclusion that the CC and the CC-SOS2 methods are the better choices for linearizing the nonlinear AEL model.

A further interesting observation is the impact of the number of breakpoints on the accuracy of the hydrogen production curve. As can be seen in **Figure 2**, increasing the number of breakpoints does not noticeably improve the accuracy of the curve, which is somehow unexpected. This behavior can be explained by the fact that the univariate nonlinear terms might exhibit only mild nonlinearities within the specified variable bounds. Future investigations will be carried out to understand this behavior in more detail.

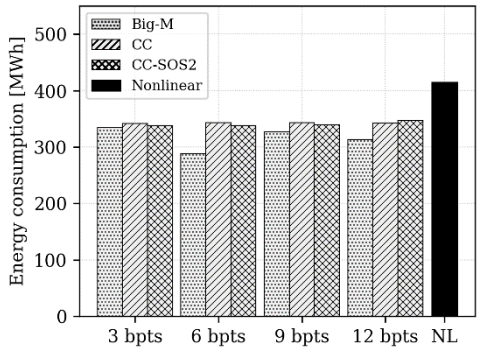

Figure 4. Total energy cosumption over a 15-hour period: MILP formulations vs. NLP.

We also see from both **Figure 2** and **Figure 3** that regardless of the linearization method used, compared to the NLP, the MILP formulations always underestimate the power consumption per kilogram of hydrogen produced. The constraints for the hydrogen production (equation 9) and the power consumption (equation 11) contain bilinear and trilinear terms, which were relaxed in the MILP using McCormick envelope. Since the McCormick relaxation provides an outer approximation of a multilinear term, the relaxation can lie below the actual function value causing the underestimation. This is further evident in the total energy consumption of the AEL over the 15-hour

optimization period, shown in **Figure 4**. However, a partitioned McCormick envelope, that will be implemented in the future, could provide a more accurate approximation.

Finally, we examine the total computational time of the different solution approaches. From **Table 2** we see that CC-SOS2 performs the fastest when having three breakpoints. However, as the number of breakpoints increases, the computational time of CC-SOS2 grows more rapidly than that of the standard CC formulation, making CC the more flexible option. As discussed previously, the Big-M method with more than three breakpoints does not produce satisfactory results. Therefore, its computation times are not considered meaningful for comparison. The reported MILP solution times were consistent across multiple runs. In contrast, the time taken for each run of the NLP varies widely with the multi-start strategy taking a total of 257 seconds for 50 runs. This wide spread of the objective values, ranging from 7909.76 to 28620.28, indicates the presence of local optima and makes it difficult to estimate in advance how many runs are required to reliably identify the best solution. Advanced optimization algorithm, such as BO-IPOPT [16, 17], which is a hybrid algorithm based on Bayesian optimization and IPOPT, will be employed in future work to address this issue.

Table 2: Solution times of the MILP formulations and the NLP.

Method	Solution time (seconds)
CC (3 breakpoints)	1.12
CC (6 breakpoints)	10.08
CC (9 breakpoints)	54.45
CC (12 breakpoints)	100.19
CC-SOS2 (3 breakpoints)	0.92
CC-SOS2 (6 breakpoints)	33.95
CC-SOS2 (9 breakpoints)	101.37
CC-SOS2 (12 breakpoints)	148.47
Big-M (3 breakpoints)	1.72
Big-M (6 breakpoints)	7.45
Big-M (9 breakpoints)	9.96
Big-M (12 breakpoints)	40.39
NLP	0.82-61.14 (single run) 257.03 (50 runs)

CONCLUSION

This study addresses a major challenge of integrating a nonlinear AEL model into a linear optimal dispatch problem of a renewable powered industrial AEL system. Two approaches were taken and compared. The first approach includes solving the operational optimization problem as an NLP by relaxing the binaries and integers within the model to continuous variables and then adding associated penalty terms to promote integrality. The NLP is then run using a multi-start strategy from random initial points. The minimum objective value is taken as the best guess for the global minimum. The second approach formulates the optimal dispatch problem as an MILP by linearizing the univariate nonlinear terms within the AEL model using piecewise approximation and relaxing the multilinear terms using McCormick envelope. The hydrogen production curve of the NLP is taken as reference since the NLP uses the original nonlinear AEL model.

We see that out of the three piecewise linearization methods, namely, CC, CC-SOS2 and big-M formulation, CC and CC-SOS2 perform very similarly in reproducing the hydrogen production curve irrespective of the number of breakpoints. The big-M method performs well only with three breakpoints. Beyond three breakpoints, choosing the big-M value becomes significantly difficult, requiring large values, and producing unusable results.

Another important, albeit surprising, observation is that increasing the number of breakpoints does not have any meaningful impact on the accuracy of the solution, possibly due to the univariate nonlinear terms within the AEL model exhibiting mild nonlinearities within the specified variable bounds.

Furthermore, we see that the MILP always underestimates the power consumption of the AEL when compared to the NLP. The McCormick relaxations of the hydrogen production and power consumption constraints can be attributed to this underestimation.

Finally, when taking a look at the computational times, we observe that the CC method is generally the fastest when working with a varied number of breakpoints. While the CC-SOS2 is marginally faster when having three breakpoints, the computational time increases much faster as the number of breakpoints increases making CC the more flexible option. We consider the big-M method not suitable for this optimization problem as it cannot produce usable results when more than three breakpoints are used and exhibits the longest computation time even in the three-breakpoint case. Comparing the computation time of the MILP with the NLP is difficult as the NLP is modeled with a multi-start approach with the time taking for each run varying widely. The presence of local optima in the NLP means it is hard to estimate how many runs are necessary to reliably obtain the best solution.

Future work includes potentially increasing the accuracy of the linearized AEL model by using the partitioned McCormick envelope that yields a tighter relaxation of multilinear terms by subdividing the variable bounds into smaller intervals. Furthermore, the MILP approach will be compared with global hybrid modeling approaches, e.g., BO-IPOPT [16, 17], and investigated as a potential initialization scheme for these hybrid methods. Additionally, these models will be validated with real data from a real plant before being evaluated for real-time digital twin implementation

ACKNOWLEDGEMENTS

The authors acknowledge the funding provided through the Establishing **E**uropean **P**roduction of **HY**drogen **R**enew**A**ble energy and integration into an industrial environment (EPHYRA) project, supported by the Clean Hydrogen Partnership in collaboration with Hydrogen Europe and Hydrogen Europe Research, under Grand Agreement no. 101112220.

AUTHOR IDENTIFIERS

Jonaed Bin Mustafa Kamal: 0009-0001-8155-0471
Loukas Kyriakidis: 0009-0003-6634-8579
Saskia Bublitz: 0000-0002-9050-7862
Bogdan Dorneanu: 0000-0003-3553-6625
Harvey Arellano-Garcia: 0000-0002-8297-0232

REFERENCES

1. Matute G, Yusta JM, Beyza J, Correas LC. Multi-state techno-economic model for optimal dispatch of grid connected hydrogen electrolysis systems operating under dynamic conditions. International Journal of Hydrogen Energy 46:1449-1460 (2021). https://doi.org/10.1016/j.ijhydene.2020.10.019
2. Bolívar Jaramillo L, Weidlich A. Optimal microgrid scheduling with peak load reduction involving an electrolyzer and flexible loads. Applied Energy 169:857-865 (2016). https://doi.org/10.1016/j.apenergy.2016.02.096
3. Korpas M, Holen AT. Operation planning of hydrogen storage connected to wind power operating in a power market. IEEE Trans. On Energy Conversion 21:742-749 (2006). https://doi.org/10.1109/tec.2006.878245
4. Baumhof MT, Raheli E, Johnsen AG et al. Optimization of hybrid power plants: when is a detailed electrolyzer model necessary? https://doi.org/10.48550/arXiv.2301.05310 (2023)
5. Hu S, Guo B, Ding S, Yang F, Dang J, Liu B, Gu J, Ma J, Ouyang M. A comprehensive review of alkaline water electrolysis mathematical modeling. Applied Energy 327:120099 (2022). https://doi.org/10.1016/j.apenergy.2022.120099
6. Ulleberg O. Modeling of advanced alkaline electrolyzers: a system simulation approach. International Journal of Hydrogen Energy 28:21-33 (2003). https://doi.org/10.1016/s0360-3199(02)00033-2
7. Sánchez M, Amores E, Rodríguez L, Clemente-Jul C. Semi-empirical model and experimental validation for the performance evaluation of a 15 kw alkaline water electrolyzer. International Journal of Hydrogen Energy 43:20332-20345 (2018). https://doi.org/10.1016/j.ijhydene.2018.09.029
8. Wächter A, Biegler LT. On the implementation of an interior-point filter line-search algorithm for large-scale nonlinear programming. Math. Program. 106:25-57 (2005). https://doi.org/10.1007/s10107-004-0559-y
9. Dantzig G. Linear programming and extensions. RAND Corporation (1963). https://doi.org/10.7249/r366
10. EPHYRA. http://www.ephyraproject.eu
11. Lin MH, Carlsson JG, Ge D, Shi J, Tsai JF. A review of piecewise linearization methods. Mathematical Problems in Engineering 2013:1-8 (2013). https://doi.org/10.1155/2013/101376
12. McCormick GP. Computability of global solutions to factorable nonconvex programs: part i — convex underestimating problems. Mathematical Programming 10:147-175 (1976). https://doi.org/10.1007/bf01580665
13. Zheng Y, You S, Bindner HW, Münster M. Optimal day-ahead dispatch of an alkaline electrolyser system concerning thermal–electric properties and state-transitional dynamics. Applied Energy 307:118091 (2022). https://doi.org/10.1016/j.apenergy.2021.118091
14. Kyriakidis L, Kansara R, Roldán Serrano MI. Energy management of industrial energy systems via rolling horizon and hybrid optimization: a real-plant application in germany. Energies 18:3977 (2025). https://doi.org/10.3390/en18153977
15. Lemmon EW, Huber ML, Leachman JW. Revised standardized equation for hydrogen gas densities for fuel consumption applications. J. Res. Natl. Inst. Stand. Technol. 113:341 (2008). https://doi.org/10.6028/jres.113.028
16. Kyriakidis L, Mendez MA, Bähr M. A hybrid algorithm based on bayesian optimization and interior point optimizer for optimal operation of energy conversion systems. Energy 312:133416 (2024). https://doi.org/10.1016/j.energy.2024.133416
17. Kyriakidis L, Bähr M, Mendez MA. Enhanced hybrid algorithm based on bayesian optimization and interior point optimizer for constrained optimization. Optim Eng : (2025). https://doi.org/10.1007/s11081-025-09975-y